Temperature-Induced Dissociation of Protein Aggregates: Accessing the Denatured State†

Filip Meersman‡ and Karel Heremans*

Department of Chemistry, Katholieke Universiteit Leuven, Celestijnenlaan 200D, B-3001 Leuven, Belgium

Received September 9, 2003; Revised Manuscript Received October 9, 2003

ABSTRACT: The thermal denaturation of lysozyme and ribonculease A (RNase A) under reducing and nonreducing conditions at neutral pH has been monitored by Fourier transform infrared spectroscopy. In the absence of the reductant, lysozyme and RNase A undergo apparent three- and two-state denaturation, respectively, as observed from the conformation-sensitive amide I′ band. For both proteins the hydrogen−deuterium exchange takes place at lower temperatures than the main denaturation temperatures, suggesting that a transient denaturation mechanism occurs. The observed transition at 51.2 °C during the denaturation of lysozyme is attributed to this transient effect, rather than to the loss of tertiary structure. Under reducing conditions lysozyme aggregates during the heating phase, whereas RNase A shows only a minor aggregation, which further increases during the cooling step. The reduced stability of both proteins can be correlated with the transient denaturation behavior, which is also suggested to be involved in protein aggregation at physiologically relevant temperatures. In addition, it is shown that when the temperature is further increased, the amorphous aggregates dissociate. Comparison of the dissociated states with the denatured states obtained under nonreducing conditions indicates that these states have the same conformation. By using a two-dimensional correlation analysis we were able to show that the dissociation is preceded by a conformational change. It is argued that this extends to other types of perturbation.

Protein aggregation is a major topic in protein chemistry because of its immense human and economic consequences (*1*). The aggregation can be due to misfolding or can be caused by different kinds of stress that partially denature the protein, which is then kinetically trapped in an aggregated state (*2*, *3*). Temperature is well established as such a stress factor that can lead to aggregation. However, little attention has been paid to high temperature as a factor causing dissociation of protein aggregates. Temperature-induced aggregate dissociation has previously been reported for the amorphous aggregates of ferrous horseradish peroxidase (*4*) and fibronectin type III module (*5*), as well as for the fibrillar aggregates of a number of peptides, including amyloid A (*6*−*8*). Despite these studies the mechanistic and structural aspects of the dissociation process still remain unclear. For instance, an intriguing question that arises is what conformation the protein will adopt after temperature-induced dissociation? Will it be a partially denatured state, i.e., the state that originally aggregated, or a fully denatured state?

In contrast to temperature, high hydrostatic pressure has long been known for its dissociating effect on native oligomeric proteins (*9*). More recently, it was also shown that pressure can dissociate temperature-induced protein aggregates (*10*−*13*). Furthermore, the heat-shock protein Hsp104 has been shown to rescue proteins from aggregates (*14*) and so do site-directed monoclonal antibodies (*15*). Reversal of aggregation under folding conditions is of great use in biotechnology, where it can increase the yield of recovery of native protein from inclusion bodies. It may also provide clues of therapeutic interest for amyloid diseases (*15*).

Fourier transform infrared spectroscopy (FTIR)[1] is a particularly useful technique to study protein aggregation or disaggregation because these processes are often characterized by the appearance or disappearance of two absorbance bands around 1615 and 1683 cm^{-1}. These two bands are indicative of intermolecular antiparallel β-sheet aggregation (*16*−*18*). On the other hand, infrared thermal denaturation studies usually result in the formation of an aggregate due to the high protein concentrations used (*19*). As the aggregation is due to the self-assembly of a partially denatured species (*2*, *3*) and the spectral features of this aggregate are dominated by the presence of two bands typical of the aggregation, one cannot obtain any structural information about the denatured state.

Aggregate dissociation could make the denatured state accessible for characterization by FTIR. To this end we investigate the thermal behavior of lysozyme and ribonuclease A under nonreducing and reducing conditions with FTIR spectroscopy. These two disulfide bond-containing proteins are, together with horseradish peroxidase, staphylococcal nuclease, and the ribonucleases S and T1, exceptional in the sense that they do not aggregate at the high

† The results presented in this paper were obtained with the support of the Research Fund of the Katholieke Universiteit Leuven and the Fonds voor Wetenschappelijk Onderzoek Vlaanderen, Belgium.

* Corresponding author: e-mail Karel.Heremans@fys.kuleuven.ac.be; tel (0032) 16-32-71-59; fax (0032)16-32-79-82.

‡ Present address: Department of Chemistry, University of Cambridge, Lensfield Road, Cambridge CB2 1EW, U.K.

[1] Abbreviations: FTIR spectroscopy, Fourier transform infrared spectroscopy, 2D-IR, two-dimensional infrared correlation spectroscopy, H/D exchange, hydrogen−deuterium exchange; D_N, denatured state under native conditions; D_R, denatured state under reducing conditions.

10.1021/bi035623e CCC: $25.00
Published on Web 11/13/2003

concentrations required for FTIR experiments (*4*, *18*−*22*). Thus, for these proteins the heat-denatured state can be characterized. However, reduction of the disulfide bonds is known to result in rapid aggregation. We observe that under reducing conditions temperature-induced aggregation and subsequent dissociation of the aggregates at higher temperatures takes place. We propose that the dissociation is due to a conformational change of the aggregated species. The dissociated state is shown to resemble the denatured state obtained under nonreducing conditions.

EXPERIMENTAL PROCEDURES

Sample Preparation. Lysozyme from chicken egg white (E.C. 3.2.1.17) and bovine pancreatic ribonuclease A (E.C. 3.1.27.5) were purchased from Sigma (St. Louis, MO) and used without further purification. The proteins were dissolved in 10 mM deuterated Tris-HCl buffer (pD 7.6) to obtain a concentration of ~3.5 mM. Reducing conditions are obtained by addition of 2-mercaptoethanol (pro analysi, Merck, Darmstadt, Germany) to the protein solution at a concentration of 0.35 M. In all cases the protein solutions were stored overnight to ensure sufficient H/D exchange of all solvent-accessible protons.

Temperature Denaturation. After centrifugation at 12100*g* for 10 min, the lysozyme and ribonulease A solutions were pipetted into a temperature cell with two CaF_2 windows (Graseby Specac, Orpington, U.K.) with a 50 μm Teflon spacer in between. The temperature cell was placed into a heating jacket, which is controlled by a Graseby Specac automatic temperature controller. The temperature increment was 0.2 °C/min and the cooling rate was 1 °C/min, unless mentioned otherwise.

FTIR Spectroscopy. Infrared spectra were recorded with a Bruker IFS66 FTIR spectrometer equipped with a liquid nitrogen-cooled mercury−cadmium−telluride solid-state detector. The sample compartment was continuously purged with dry air. Two hundred and fifty interferograms were coadded after registration with a resolution of 2 cm^{-1}.

Fourier Self-Deconvolution. Resolution enhancement was achieved by Fourier self-deconvolution, a mathematical technique of band narrowing, and was performed with the Bruker software. The assumed line shape was Lorentzian. A half bandwidth of 21 cm^{-1} and an enhancement factor of 1.7 were used. The meaning of these parameters, as well as the possible difficulties of deconvolution, have been discussed elsewhere (*23*).

Fitting. The secondary structure was determined by fitting the self-deconvoluted amide I band of the spectrum by use of Gaussian functions (*24*, *25*). The fitting of component peaks was performed by a program developed in our laboratory, using the Levenberg−Marquardt algorithm (*26*).

Two-Dimensional IR Correlation Spectroscopy. The 2D correlation methodology is based on the comparison of the intensity changes as a function of perturbation parameter at two distinct and independent wavenumbers. This comparison is achieved by Fourier-transforming the temperature variable as follows (*27*):

$$Y(\nu, \omega) = \int_{-\infty}^{+\infty} y(\nu, T) e^{-i\omega T}\, dT \qquad (1)$$

where ν and ω are the spectral and Fourier frequencies, respectively, T is the temperature, and $y(\nu, T)$ represents the dynamic intensity fluctuations. This transformation is followed by calculating the correlation between $Y(\nu_1,\omega)$ and $Y^*(\nu_2,\omega)$:

$$\phi(\nu_1, \nu_2) + i\psi(\nu_1, \nu_2) = (\pi\Delta T)^{-1} \int_{-\infty}^{+\infty} Y(\nu_1, \omega_1) Y^*(\nu_2, \omega_2)\, d\omega \qquad (2)$$

where $\phi(\nu_1, \nu_2)$ is the real part of the correlation intensity and $\psi(\nu_1, \nu_2)$ is the imaginary part, and ΔT is the temperature interval. Plotting these parts in the (ν_1, ν_2) plane results in a synchronous and an asynchronous plot, respectively.

Synchronous plots highlight the spectral changes that are *in phase* and thus recognize similarities between the two intensities that are considered. In contrast, asynchronous plots show *out-of-phase* changes. In this case the cross-peaks are formed only between those bands whose intensity evolves independently as a function of temperature (*28*).

In practice, the synchronous and asynchronous correlation plots are calculated starting from the original (not band-narrowed) absorption spectra with a program written by Dr. L. Smeller (Budapest). In the correlation plots, positive peaks are white, and negative peaks are darkened. In the synchronous plot a positive cross-peak at (ν_1, ν_2) indicates that the induced changes in intensity at these wavenumbers are in the same direction. In the asynchronous plot a positive cross-peak at (ν_1, ν_2), where $\nu_1 < \nu_2$, suggests that the intensity change at ν_1 precedes the change at ν_2 and vice versa for a negative correlation peak.

RESULTS

Temperature Effect on Lysozyme under Nonreducing Conditions. Figure 1A shows the deconvoluted amide I′ band of lysozyme as a function of temperature. The change in intensity of the band at 1652 cm^{-1}, assigned to α-helix (*24*, *29*), is plotted in Figure 1B. Two transitions can be observed at 51.2 ± 0.2 and 73.2 ± 0.5 °C, respectively. The first transition coincides with the transition of the H/D exchange ($T_{1/2}$ = 52.5 ± 0.3 °C), which causes a small shift of the composing amide I′ bands. This can be seen from the ratio of the intensities of the 1450 and 1550 cm^{-1} bands, which is indicative of H/D exchange (Figure 1B). Furthermore, the spectra show an intensity increase of the bands at 1665 and 1641 cm^{-1} (Figure 1A). These have been assigned to turn structures (*24*, *29*) and 3_{10}-helix (*28*, *30*), respectively. The second transition corresponds to the denaturation. At 78 °C a plateau is obtained (Figure 1B) and the broad featureless band is characteristic for the denatured state, from here on referred to as D_N (Figure 1A).

During the consecutive cooling, two new bands start developing around 75 °C at 1615 and 1683 cm^{-1} (Figure 1A). The formation of these two bands is typical for intermolecular antiparallel β-sheet aggregation (*16*−*18*). The experiment was reproduced several times and the aggregation bands always appeared at 75 °C, in the cooling phase. The aggregation is the result of a kinetic competition between the formation of a hydrophobic core and aggregation during refolding (*31*).

When the protein sample is reheated after return to ambient conditions (25 °C), the aggregation bands start to decrease at 70 °C, indicating dissociation (data not shown). However,

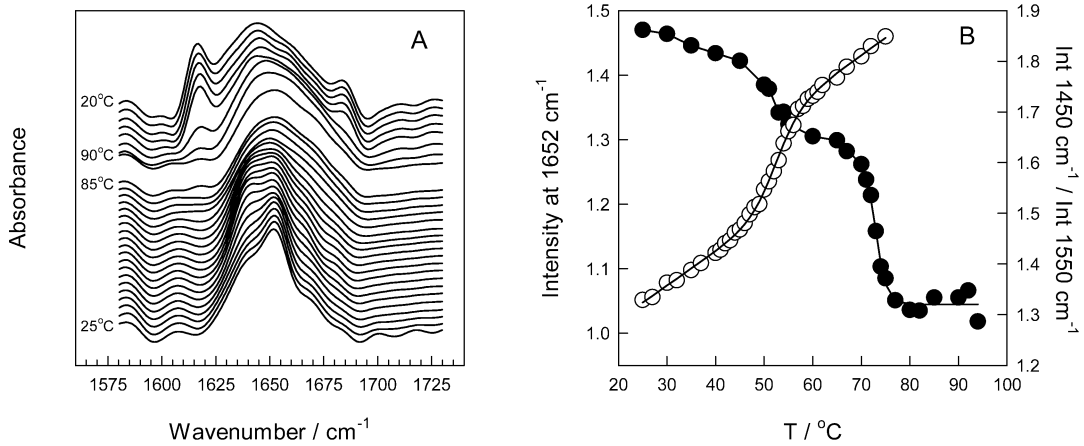

FIGURE 1: Temperature dependence of lysozyme under nonreducing conditions. (A) Stacked plot of the deconvoluted amide I′ band. Spectra are shown at 25, 30, 35, 40, 45, 50, 53, 55, 60, 65, 70, 71, 72, 73, 74, 75, 80, and 85 °C for the heating phase. In the cooling phase the temperature decreases in steps of 10 °C. (B) Temperature dependence of the intensity of the α-helix band at 1652 cm^{-1} (●) and H/D exchange of native lysozyme with increasing temperature (○). The ratio 1450 cm^{-1}/1550 cm^{-1} is typical of the amount of hydrogens exchanged for deuterons.

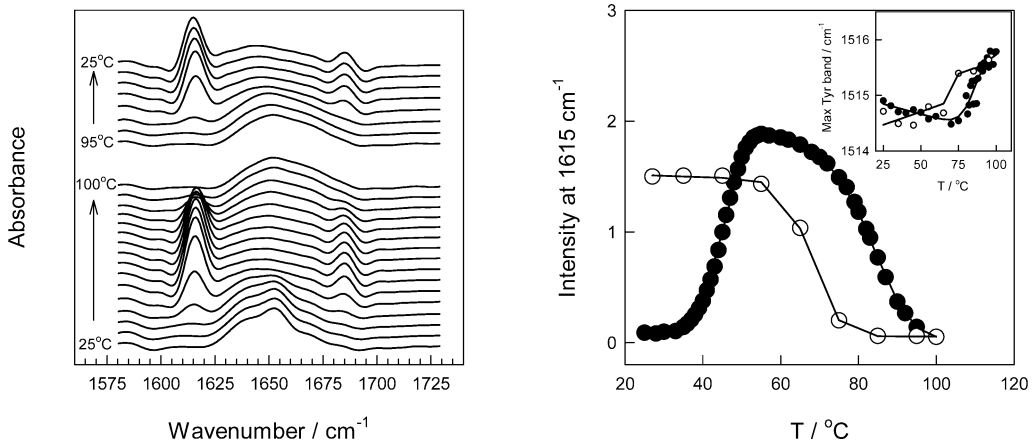

FIGURE 2: Temperature dependence of lysozyme under reducing conditions. (A) Stacked plot of the deconvoluted amide I′ region. Temperature increases/decreases in steps of 5/10 °C from bottom to top. (B) Intensity of the 1615 cm^{-1} band, characteristic of aggregation, versus temperature. Inset: temperature dependence of the tyrosine band maximum. Heating (●), cooling (○).

these bands do not completely disappear at 85 °C, suggesting that higher temperatures are required to induce a complete dissociation. In the following cooling step the aggregation bands at 1615 and 1683 cm^{-1} reappear.

The position of the tyrosine band maximum (around 1515 cm^{-1}) as a function of temperature does not change up to 70 °C (data not shown). Above 70 °C the band maximum shows a typical shift to higher wavenumber. This suggests that the tyrosine environment remains intact at 50 °C but becomes solvent-exposed at 75 °C.

Temperature Effect on Lysozyme under Reducing Conditions. Under reducing conditions the thermal denaturation of lysozyme readily results in the formation of an aggregate (Figure 2A), without the formation of an observable intermediate state. Figure 2B shows the band intensity at 1615 cm^{-1} as a function of temperature, which originates from the intermolecular antiparallel β-sheet aggregation. At 35 °C the intensity of this band starts to increase and the midpoint of this transition, $T_{1/2}$, is found at 46.0 ± 0.2 °C. This is roughly the same temperature as for the H/D-exchange transition midpoint under nonreducing conditions. Thus, the reduction of the disulfide bonds causes a drastic decrease in temperature stability by almost 30 °C compared to the native lysozyme (Figure 1B). Above 70 °C the IR aggregation bands start to disappear ($T_{1/2}$ = 86.4 ± 0.7 °C). At 100 °C these bands are completely absent in the amide I′ region, indicating that the dissociation has come to an end. The denatured state obtained is referred to as D_R. Upon returning back to room temperature the aggregation bands reappear ($T_{1/2}$ = 67.9 ± 0.4 °C) (Figure 2).

To get a better insight into the dissociation process we performed a 2D-IR analysis, which can reveal the sequence of events induced by a perturbation, in casu temperature. For instance, it has been applied to identify the processes underlying protein denaturation (*27*) and aggregation (*32*). Synchronous and asynchronous correlation plots were generated in the temperature region where the dissociation occurs (between 68 and 100 °C) and are shown in Figure 3. The synchronous plot shows that major intensity changes occur around 1615 and 1645 cm^{-1}. The former is characteristic of β-sheet aggregation, whereas the latter results from non-β-sheet structures. It can be seen that the 1645 cm^{-1} band represents a rather broad area that does not display any well-resolved bands, likely because it is composed of a number of overlapping bands. The presence of a negative cross-peak between the 1615 cm^{-1} band and this area indicates that the intensity changes occur in opposite directions. Figure 2 clearly demonstrates a drop in the intensity of the 1615 cm^{-1}

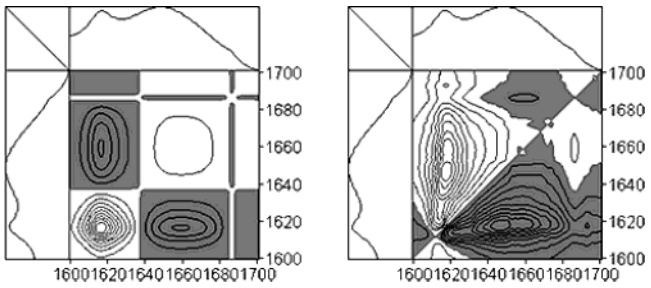

FIGURE 3: Two-dimensional correlation plots of the amide I′ band of lysozyme between 68 and 100 °C (under reducing conditions). Synchronous, left panel; asynchronous, right panel. Nondeconvoluted spectra were used.

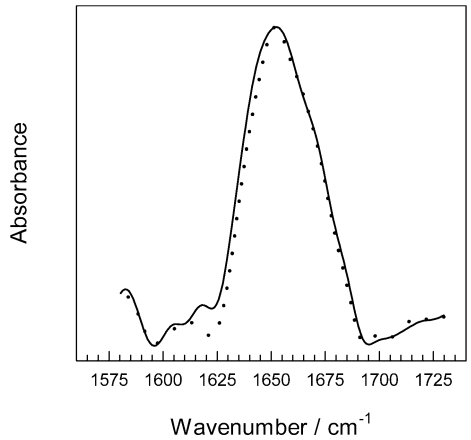

FIGURE 4: Superposition of the deconvoluted amide I′ band of the denatured states of lysozyme under nonreducing (solid line) and reducing (dotted line) conditions. The spectra were normalized to the same intensity.

band. The negative cross-correlation in the asynchronous plot suggests that the increase in intensity in the 1640−1680 cm^{-1} area starts to occur before the intensity of the aggregation band around 1615 cm^{-1} starts to decrease.

The position of the tyrosine band is plotted versus temperature in Figure 2B (inset). The band position does not change during the aggregation but shifts to a higher wavenumber during the dissociation. The band shift is reversible, albeit with a significant hysteresis, which is also observed for the plot of the intensity at 1615 cm^{-1} (Figure 2B). The hysteresis could be due to a difference in the heating and cooling rates or it could be that a partial refolding is required prior to the aggregation. Moreover, it can be seen that the onset temperature of dissociation equals the onset temperature of reaggregation. This suggests that under the given conditions the aggregates are not stable above this temperature, and therefore will not form.

Comparison of D_N and D_R. Figure 4 shows a superposition of the deconvoluted amide I′ region of D_N and D_R, the denatured states obtained under nonreducing and reducing conditions, respectively. It can be seen that these spectra do not significantly differ from one another. Note that the spectra lack a significant absorption in the 1620−1640 cm^{-1} area where β-sheet contributions are usually found. This provides further evidence of a complete dissociation.

Temperature Effect on Ribonuclease A under Reducing Conditions. To check whether the above results can be extended to other proteins, we performed similar experiments on RNase A. Basically we find the same aggregation−dissociation behavior as for lysozyme. This is summarized in Figure 5, which shows the effect of heating to 75 °C, cooling back to room temperature (25 °C), and a second heating−cooling cycle (25 → 100 → 25 °C). There are, however, some notable differences compared to lysozyme. (i) RNase A denatures around 60 °C in the presence of mercaptoethanol, which is only 7 °C less stable than the native protein. For comparison the thermally induced changes in the amide I′ and II/II′ areas under nonreducing conditions have been plotted in Figure 6 (see Discussion). (ii) The denaturation is accompanied by a minor intensity increase of the band at 1616 cm^{-1} (Figure 7). This suggests that only part of the molecules aggregates. Only during the cooling phase do the aggregation bands fully develop.

As shown in Figure 5B, the spectral features of denatured RNase A under reducing and nonreducing conditions are very similar, which confirms earlier findings (*33* and references therein).

DISCUSSION

Temperature-Induced Transient Denaturation of Lysozyme. The fact that the H/D exchange is completed at temperatures below the denaturation transition temperature was interpreted by van Stokkum et al. (*19*) as a loss of tertiary structure. Because the secondary structure remained intact, these authors concluded that an intermediate was formed. However, H/D exchange can also result from a more transient process, causing local, subglobal, or global denaturation (*34*). We

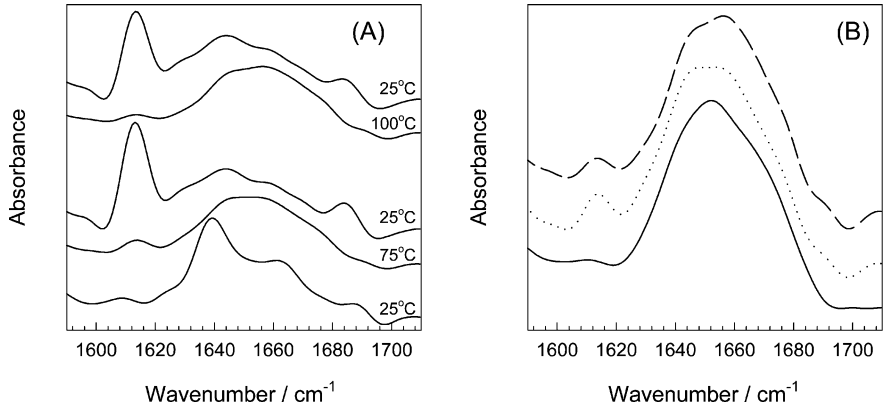

FIGURE 5: Thermal behavior of RNase A. (A) Deconvoluted amide I′ region of RNase A at various temperatures under reducing conditions. (B) Comparison of the denatured state under nonreducing conditions (at 100 °C) with the dissociated states of RNase A at 75 and 100 °C, under reducing conditions (sequence from bottom to top).

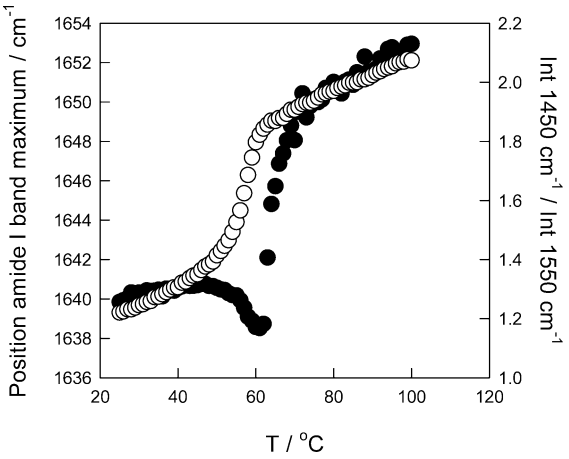

FIGURE 6: Temperature dependence of the band characteristics of RNase A under nonreducing conditions. Position of the amide I′ band maximum (●); ratio of the intensities at 1450 and 1550 cm^{-1}, indicative of H/D exchange (○).

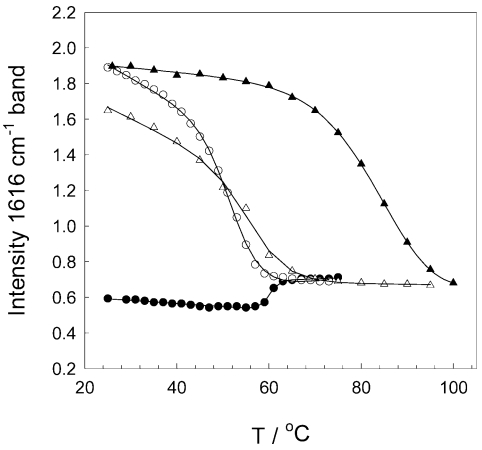

FIGURE 7: Intensity of the 1616 cm^{-1} band for RNase A under reducing conditions during two heating−cooling cycles. Circles, first cycle; triangles, second cycle. Solid symbols, heating; open symbols, cooling. The heating/cooling rate was 0.5 °C/min.

favor the latter view, i.e., the absence of an intermediate, which is supported by a variety of techniques including nuclear magnetic resonance (*35*), circular dichroism (*36*), FTIR spectroscopy (*18*), and molecular dynamics simulations (*37*). Furthermore, it was shown by Radford et al. (*35*) that at elevated temperature a large-scale denaturation is the likely mechanism of exchange for lysozyme. This suggests that the first transition that can be seen for lysozyme around 50 °C (Figure 1B) is likely to be an artifact of the exchange, rather than a conformational change. This is supported by the observed changes in tyrosine environment. Lysozyme contains three tyrosine residues (Tyr20, Tyr23, and Tyr53). The first two are located in the α-domain of the protein, while the latter is part of a strand in the *β*-domain. The absorption band of the tyrosine residues can be found outside the amide I′ band at 1515 cm^{-1} (*38*). When a protein denatures and the tyrosine residues become solvent-exposed, the tyrosine band shifts toward a higher wavenumber (*20*, *21*). This is not observed below 70 °C.

The transient denaturation also makes the disulfide bonds accessible to the solvent, thereby causing their reduction. Subsequently, the reduced lysozyme aggregates, which is not surprising as it is known that reduced lysozyme is highly aggregation-prone (*31*, *39*). This is evident from the correlation between the H/D exchange and aggregation onset temperatures.

Interestingly, Dong et al. (*18*) succeeded in populating an intermediate on the thermal denaturation pathway of lysozyme in the presence of low concentrations of guanidine hydrochloride. Similarly, Mark and Van Gunsteren (*37*) managed to stabilize the transient intermediate state by cooling the system in a molecular dynamics simulation. This suggests that given the right conditions the transient denaturation behavior might lead to the population of intermediate states, which is particularly interesting from the viewpoint of protein aggregation. Indeed, one of the conditions that most readily results in the formation of human wild-type lysozyme fibrils is at pH 2 and 57 °C (*40*), which is the temperature region where we observe a transient global denaturation of egg white lysozyme. Thus, such conformational fluctuations might, under conditions of, e.g., overexpression, lead to the formation of aggregates. For a number of proteins that are involved in conformational diseases this might happen within the range of the body temperature. For example, amyloidogenic lysozyme variants exhibit nearly complete H/D exchange at 37 °C (*41*). A similar idea has been put forward by Balbirnie et al. (*42*). However, Chamberlain et al. (*43*) have pointed out that although mutations in the structure of lysozyme can change both the dynamics of the native state and the ability to access partially denatured states, it is the latter that appears to be the origin of the amyloidogenic nature of the mutants. In our opinion, the flexibility and the ability to populate partially denatured conformations are interrelated.

A Thermal Denaturation Intermediate for RNase A? Similar to lysozyme, it has been argued that the occurrence of the H/D exchange at a temperature below the main denaturation temperature is due to the loss of tertiary structure. However, techniques such as nuclear magnetic relaxation dispersion (*44*) and solution X-ray scattering (*45*) do not indicate the existence of a molten globule-like intermediate state. On the basis of our FTIR experiments we believe that a transient denaturation mechanism explains this phenomenon as well. Recently, Navon et al. (*46*) detected transition temperatures at 58 and 63 °C by UV and CD spectroscopy, respectively. These temperatures are in agreement with those found in this work under nonreducing conditions. Although UV absorbance monitors changes in tertiary structure, Navon et al. (*46*) showed that mainly long-range interactions are weakened and that further disruption of the tertiary contacts takes place at higher temperatures. Their observations therefore do not contradict the notion of a transient global denaturation event.

Such a mechanism also rationalizes the relatively small difference in temperature stability of RNase A under nonreducing and reducing conditions. Although analysis of the spectral changes in the amide I′ band indicates a two-state mechanism, it can be seen that the H/D exchange takes place at temperatures below the denaturation transition (Figure 6). Since the two disulfide bonds (Cys26−Cys84 and Cys58−Cys110) that contribute mostly to the conformational stability of RNase A are deeply buried within the hydrophobic core (*33*, *47*) these will not be reduced until the protein structure unfolds, either transiently or nontransiently. The denaturation temperature under reducing conditions ($T_{1/2}$ =58 ± 0.2 °C) approximately equals the temperature for the H/D exchange under both reducing ($T_{1/2}$ = 54.8 ± 0.2 °C) and nonreducing

($T_{1/2} = 57.2 \pm 0.1$ °C) conditions. This suggests that RNase A unfolds as soon as its disulfide bonds are reduced. Because these are fairly protected within the protein, the destabilization is less than in the case of lysozyme.

Temperature-Induced Dissociation. Reduction of the disulfide bonds in lysozyme and RNase A enables us to induce aggregation and dissociation within a reasonable temperature interval (<100 °C). We observe that the dissociation, i.e., the disappearance of the aggregation bands around 1615 and 1683 cm^{-1}, is simultaneously accompanied by (i) changes in the amide I′ region between these two bands, which indicate the conversion of β-sheet structure into disordered structure and loop structures, rather than a mere disruption of the intermolecular interactions, which would result in the retention of a high β-sheet content; and (ii) changes in tyrosine environment, which is a marker for tertiary contacts. This suggests that the dissociation is accompanied by or results from a conformational change, i.e., further denaturation, of lysozyme. Although it is difficult to discriminate between these two options, it should be emphasized that the 2D-IR correlation plots indicate that, prior to the disappearance of the aggregation bands, conformational rearrangements take place in the non-β-sheet structural elements of the protein, which eventually result in the dissociation of the aggregate. This suggests that the main driving force for dissociation is a conformational change. Additional support for this hypothesis is provided by the fact that, in the case of lysozyme, the onset temperature of dissociation is approximately 70 °C (Figure 2B), where the hydrophobic interaction is known to be strongest (*48*). Thus, the dissociation cannot be ascribed to a weakening of the hydrophobic interaction. Moreover, protein dissociation or inhibition of aggregation can be induced by other factors, including antibodies (*15*, *49*), molecular chaperones (*14*, *50*), high hydrostatic pressure (*10*−*13*), and small compounds such as melatonin (*51*) or β-sheet breaker peptides (*52*). Antibodies, for instance, interact with a specific epitope on a protein instead of affecting the whole molecule. This implies that their action has to be transmitted throughout the molecule in order to cause dissociation, which can only be achieved by a conformational change. It is known that antibody−antigen interactions involve conformational changes, the magnitude of which can vary from insignificant to considerable (*15*). Therefore, we put forward the hypothesis that the above phenomena can be interpreted by assuming a common mechanism, being the induction of a conformational change or, in case of inhibition, the stabilization of a nativelike conformation. In the particular case of high hydrostatic pressure, our hypothesis is supported by NMR data that indicate the existence of a *predissociation conformational change* in the pressure-induced dissociation of the dimeric Arc repressor (*53*).

A comparison of D_N and D_R suggests that the secondary structure of these states is the same. Thus, the dissociation of an aggregate results in the formation of a denatured state, rather than in the reversal of the aggregation process. The latter would have resulted in an aggregation-prone, intermediatelike conformation. This is in agreement with Holzbaur et al. (*4*), who showed that the infrared spectrum of ferrous horseradish peroxidase after dissociation was essentially the same as that of the ferric form, which did not aggregate during thermal denaturation. Our findings are summarized in Scheme 1:

Scheme 1

$$\begin{array}{ccc} N(\Leftrightarrow N^*) & \Leftrightarrow & D \\ \downarrow & & \Updownarrow \\ A & \Leftrightarrow & A^* \end{array}$$

where N is the native state, N* is a nativelike, expanded conformation, A is the aggregate, A* is the aggregate in which the individual molecules have undergone a conformational change, i.e., the pre-unfolded state, and D is the denatured state. Note that Scheme 1 is similar to the proposed pathway for the thermal behavior of fibronectin type III domain (*5*) but includes the existence of a pre-unfolded state A*. The expanded state, N*, has been invoked by Kendrick et al. (*54*) to explain the apparent absence of an intermediate prior to aggregation in many FTIR experiments. In this respect it is worth mentioning that the tyrosine environment does not change upon aggregation, indicating that the aggregation-prone species is not fully denatured. This is consistent with the notion that aggregation requires only a partially denatured state (*2*, *3*). Furthermore, our result supports the work of Denisov et al. (*55*), who were able to show that the denatured states of native and reduced lysozyme mainly differ in their flexibility rather than in their conformation.

In summary, we have argued that conformational fluctuations can result in the transient formation of (partially) denatured states that have a high tendency to aggregate. Because these fluctuations can take place at temperatures significantly lower than the denaturation temperature, they may explain the occurrence of disease-related aggregation at physiologically relevant temperatures. An important difference with the present view of aggregation is that this mechanism does not involve the population of a partially denatured species or that it assumes another role for this intermediate species. Indeed, Chiti et al. (*56*) have suggested that such intermediates may promote aggregation indirectly by favoring equilibria with other less structured conformations that exist only transiently and that are highly aggregation-prone. In addition, this work extends previous data on temperature-induced dissociation of protein aggregates (*4*−*8*). Taken together, the data suggest that this phenomenon is generally applicable to all proteins. The suggested role of a conformational change in the dissociation process adds further support to the view that molecules, such as antibodies, that can induce conformational changes are potential therapeutic agents for amyloid and other aggregation disorders. Moreover, temperature modulation may be a useful way to optimize the reversal of aggregation in biotechnological applications.

REFERENCES

1. De Young, L. R., Dill, K. A., and Fink, A. L. (1993) Aggregation and denaturation of apomyoglobin in aqueous urea solutions, *Biochemistry 32*, 3877−3886.
2. Fink, A. L. (1998) Protein aggregation: folding aggregates, inclusion bodies and amyloid, *Fold. Des. 3*, R9−R23.
3. Dobson, C. M. (2001) The structural basis of protein folding and its links with human disease, *Philos. Trans. R. Soc. London B 356*, 133−145.
4. Holzbaur, I. E., English, A. M., and Ismail, A. A. (1996) FTIR study of the thermal denaturation of horseradish and cytochrome *c* peroxidases in D_2O, *Biochemistry 35*, 5488−5495.

5. Litvinovich, S. V., Brew, S. A., Aota, S., Akiyama, S. K., Haudenschild, C., and Ingham, K. C. (1998) Formation of amyloid-like fibrils by self-association of a partially folded fibronectin type III module, *J. Mol. Biol. 280*, 245−258.
6. Dubois, J., Ismail, A. A., Chan, S. L., and Ali-Khan, Z. (1999) Fourier transform infrared spectroscopic investigation of temperature- and pressure-induced disaggregation of amyloid A, *Scand. J. Immunol. 49*, 376−380.
7. West, M. W., Wang, W. X., Patterson, J., Mancias, J. D., Beasley J. R., and Hecht, M. H. (1999) De novo amyloid proteins from designed combinatorial libraries, *Proc. Natl. Acad. Sci. U.S.A. 96*, 11211−11216.
8. Koscielska-Kasprzak, K., and Otlewski, J. (2003) Amyloid-forming peptides selected proteolytically from phage display library, *Protein Sci. 12*, 1675−1685.
9. Silva, J. L., and Weber, G. (1993) Pressure stability of proteins, *Annu. Rev. Phys. Chem. 44*, 89−113.
10. Gorovits, B. M., and Horowitz, P. M. (1998) High hydrostatic pressure can reverse aggregation of protein folding intermediates and facilitate acquisition of native structure, *Biochemistry 37*, 6132−6135.
11. Smeller, L., Rubens, P., and Heremans, K. (1999) Pressure effect on the temperature-induced unfolding and tendency to aggregate of myoglobin, *Biochemistry 38*, 3816−3820.
12. Foguel, D., Robinson, C. R., Caetano de Sousa, P., Jr., Silva, J. L., and Robinson, A. S. (1999) Hydrostatic pressure rescues native protein from aggregates, *Biotechnol. Bioeng. 63*, 552−558.
13. St. John, R. J., Carpenter, J. F., Balny, C., and Randolph, T. W. (2001) High-pressure refolding of recombinant human growth hormone from insoluble aggregates, *J. Biol. Chem. 276*, 46856−46863.
14. Parsell, D. A., Kowal, A. S., Singer, M. A., and Lindquist, S. (1994) Protein disaggregation mediated by heat-shock protein Hsp104, *Nature 372*, 475−478.
15. Solomon, B., Koppel, R., Frankel, D., and Hanan-Aharon, E. (1997) Disaggregation of Alzheimer β-amyloid by site-directed mAb, *Proc. Natl. Acad. Sci. U.S.A. 94*, 4109−4112.
16. Ismail, A. A., Mantsch, H. H., and Wong, P. T. T. (1992) Aggregation of chymotrypsin: portrait by infrared spectroscopy, *Biochim. Biophys. Acta 1121*, 183−188.
17. Damaschun, G., Damaschun, H., Fabian, H., Gast, K., Krober, R., Wieske, M., and Zirwer, D. (2000) Conversion of yeast phosphoglycerate kinase into amyloid-like structure, *Proteins 39*, 204−211.
18. Dong, A., Randolph, T. W., and Carpenter, J. F. (2000) Entrapping intermediates of thermal aggregation in α-helical proteins with low concentration of guanidine hydrochloride, *J. Biol. Chem. 275*, 27689−27693.
19. van Stokkum, I. H. M., Linsdell, H., Hadden, J. M., Haris, P. I., Chapman, D., and Bloemendal, M. (1995) Temperature-induced changes in protein structures studied by Fourier transform infrared spectroscopy and global analysis, *Biochemistry 34*, 10508−10518.
20. Fabian, H., Schultz, C., Naumann, D., Landt, O., Hahn, U., and Saenger, W. (1993) Secondary structure and temperature-induced unfolding and refolding of ribonuclease T1 in aqueous solution. A Fourier transform infrared spectroscopic study, *J. Mol. Biol. 232*, 967−981.
21. Torrent, J., Rubens, P., Ribo, M., Heremans, K., and Vilanova, M. (2001) Pressure versus temperature unfolding of ribonuclease A: an FTIR spectroscopic characterization of 10 variants at the carboxy-terminal site, *Protein Sci. 10*, 725−734.
22. Panick, G., and Winter, R. (2000) Pressure-induced unfolding/refolding of ribonuclease A: static and kinetic Fourier transform infrared spectroscopy study, *Biochemistry 39*, 1862−1869.
23. Smeller, L., Goossens, K., and Heremans, K. (1995) How to minimize certain artifacts in Fourier self-deconvolution, *Appl. Spectrosc. 49*, 1538−1542.
24. Byler, D. M., and Susi, H. (1986) Examination of the secondary structure of proteins by deconvolved FTIR spectra, *Biopolymers 25*, 469−487.
25. Smeller, L., Goossens, K., and Heremans, K. (1995) Determination of the secondary structure of proteins at high pressure, *Vibr. Spectrosc. 8*, 199−203.
26. Press, W. H., Flannery, B. P., Teukolsky, S. A., and Vetterling, W. T. (1986) In *Numerical recipes: the art of scientific computing*, Cambridge University Press, Cambridge, U.K., Chapter 12.6.
27. Fabian, H., Mantsch, H. H., and Schultz, C. P. (1999) Two-dimensional IR correlation spectroscopy: Sequential events in the unfolding process of the λ Cro-V55C repressor protein, *Proc. Natl. Acad. Sci. U.S.A. 96*, 13153−13158.
28. Dzwolak, W., Kato, M., Shimizu, A., and Taniguchi, Y. (2000) Comparative two-dimensional Fourier transform infrared correlation spectroscopic study on the spontaneous, pressure-, and temperature-enhanced H/D exchange in α-lactalbumin, *Appl. Spectrosc. 54*, 963−967.
29. Jackson, M., and Mantsch, H. H. (1995) The use and misuse of FTIR spectroscopy in the determination of protein structure, *Crit. Rev. Biochem. Mol. Biol. 30*, 95−120.
30. Prestrelski, S. J., Byler, D. M., and Thompson, M. P. (1991) Infrared spectroscopic discrimination between α- and 3_{10}-helices in globular proteins, *Int. J. Pept. Protein Res. 37*, 508−512.
31. Goldberg, M. E., Rudolph, R., and Jaenicke, R. (1991) A kinetic study of the competition between renaturation and aggregation during the refolding of denatured-reduced egg white lysozyme, *Biochemistry 30*, 2790−2797.
32. Paquet, M.-J., Laviolette, M., Pézolet, M., and Auger, M. (2001) Two-dimensional infrared correlation spectroscopy study of the aggregation of cytochrome *c* in the presence of dimyristoylphosphatidylglycerol, *Biophys. J. 81*, 305−312.
33. Wedemeyer, W. J., Welker, E., Narayan, M., and Scheraga, H. A. (2000) Disulfide bonds and protein folding, *Biochemistry 39*, 4207−4216.
34. Englander, S. W., Mayne, L., Bai, Y., and Sosnick, T. R. (1997) Hydrogen exchange: The modern legacy of Linderstrøm-Lang, *Protein Sci. 6*, 1101−1109.
35. Radford, S. E., Buck, M., Topping, K. D., Dobson, C. M., and Evans, P. A. (1991) Hydrogen exchange in native and denatured states of hen egg-white lysozyme, *Proteins: Struct., Funct., Genet. 14*, 237−248.
36. Matagne, A., Jamin, M., Chung, E. W., Robinson, C. V., Radford, S. E., and Dobson, C. M. (2000) Thermal unfolding of an intermediate is associated with non-Arrhenius kinetics in the folding of hen lysozyme, *J. Mol. Biol. 297*, 193−210.
37. Mark, A. E., and Van Gunsteren, W. F. (1992) Simulation of the thermal denaturation of hen egg white lysozyme: trapping the molten globule state, *Biochemistry 31*, 7745−7748.
38. Rahmelow, K., Hübner, W., and Ackermann, Th. (1998) Infrared absorbances of protein side chains, *Anal. Biochem. 257*, 1−11.
39. van den Berg, B., Ellis, R. J., and Dobson, C. M. (1999) Effects of macromolecular crowding on protein folding and aggregation, *EMBO J. 18*, 6927−6933.
40. Morozova-Roche, L. A., Zurdo, J., Spencer, A., Noppe, W., Receveur, V., Archer, D. B., Joniau, M., and Dobson, C. M. (2000) Amyloid fibril formation and seeding by wild-type human lysozyme and its disease-related mutational variants, *J. Struct. Biol. 130*, 339−351.
41. Booth, D. R., Sunde, M., Bellotti, V., Robinson, C. V., Hutchinson, W. L., Fraser, P. E., Hawkins, P. N., Dobson, C. M., Radford, S. E., Blake, C. C. F., and Pepys, M. B. (1997) Instability, unfolding and aggregation of human lysozyme variants underlying amyloid fibrillogenesis, *Nature 385*, 787−793.
42. Balbirnie, M., Grothe, R., and Eisenberg, D. S. (2001) An amyloid-forming peptide from the yeast prion Sup35 reveals a dehydrated β-sheet structure for amyloid, *Proc. Natl. Acad. Sci. U.S.A. 98*, 2375−2380.
43. Chamberlain, A. K., Receveur, V., Spencer, A., Redfield, C., and Dobson, C. M. (2001) Characterization of the structure and dynamics of amyloidogenic variants of human lysozyme by NMR spectroscopy, *Protein Sci. 10*, 2525−2530.
44. Denisov, V. P., and Halle, B. (1998) Thermal denaturation of ribonuclease A characterized by water O-17 and H-2 magnetic relaxation dispersion, *Biochemistry 37*, 9595−9604.
45. Hagihara, Y., Hoshino, M., Hamada, D., Kataoka, M., and Goto, Y. (1998) Chainlike conformation of heat-denatured ribonuclease A and cytochrome *c* as evidenced by solution X-ray scattering, *Fold. Des. 3*, 195−201.
46. Navon, A., Ittah, V., Laity, J. H., Scheraga, H. A., Haas, E., and Gussakovsky, E. E. (2001) Local and long-range interactions in the thermal unfolding transition of bovine pancreatic ribonuclease A, *Biochemistry 40*, 93−104.
47. Klink, T. A., Woycechowsky, K. J., Taylor, T. M., and Raines, R. T. (2000) Contribution of disulfide bonds to the conformational stability and catalytic activity of ribonuclease A, *Eur. J. Biochem. 267*, 566−572.
48. Daniel, R. M., Dines, M., and Petach, H. H. (1996) The denaturation and degradation of stable enzymes at high temperatures, *Biochem. J. 317*, 1−11.

49. Peretz, D., Williamson, R. A., Kaneko, K., Vergara, J., Leclerc, E., Schmitt-Ulms, G., Mehlhorn, I. R., Legname, G., Wormald, M. R., Rudd, P. M., Dwek, R. A., Burton, D. R., and Prusiner, S. B. (2001) Antibodies inhibit prion propagation and clear cell cultures of prion infectivity, *Nature 412*, 739−743.
50. Ben-Zvi, A. P., and Goloubinoff, P. (2001) Mechanisms of disaggregation and refolding of stable protein aggregates by molecular chaperones, *J. Struct. Biol. 135*, 84−93.
51. Pappolla, M., Bozner, P., Soto, C., Shao, H., Robakis, N. K., Zagorski, M., Frangione, B., and Ghiso, J. (1998) Inhibition of Alzheimer β-fibrillogenesis by melatonin, *J. Biol. Chem. 273*, 7185−7188.
52. Soto, C. (2000) Reversion of prion protein conformational changes by synthetic β-sheet breaker peptides, *Lancet 355*, 192−197.
53. Peng, X., Jonas, J., and Silva, J. L. (1993) Molten-globule conformation of Arc repressor monomers determined by high-pressure ^{1}H NMR spectroscopy, *Proc. Natl. Acad. Sci. U.S.A. 90*, 1776−1780.
54. Kendrick, B. S., Carpenter, J. F., Cleland, J. L., and Randolph, T. W. (1998) A transient expansion of the native state precedes aggregation of recombinant human interferon-gamma, *Proc. Natl. Acad. Sci. U.S.A. 95*, 14142−14146.
55. Denisov, V. P., Jonsson, B.-H., and Halle, B. (1999) Hydration of denatured and molten globule proteins, *Nat. Struct. Biol. 6*, 253−260.
56. Chiti, F., Mangione, P., Andreola, A., Giorgetti, S., Stefani, M., Dobson, C. M., Bellotti, V., and Taddei, N. (2001) Detection of two partially structured species in the folding process of the amyloidogenic protein β2-microglobulin, *J. Mol. Biol. 307*, 379−391.

BI035623E